united nations
educational, scientific
and cultural
organization

international atomic
energy agency

the
abdus salam
international centre for theoretical physics

H4.SMR/1519-1

"Seventh Workshop on Non-Linear Dynamics and
Earthquake Prediction"

29 September - 11 October 2003

On the Forward and Backward Modeling of Mantle Dynamics

Alik T. Ismail-Zadeh

International Institute of Earthquake Prediction Theory
and Mathematical Geophysics, Russian Academy of Sciences
Moscow, Russia

Now at: Institute of Geophysics, University of Karlsruhe
Karlsruhe, Germany
e-mail: Ismail-Zadeh@gpi.uni-karlsruhe.de

United Nations Educational Scientific and Cultural Organization
and
International Atomic Energy Agency

THE ABDUS SALAM
INTERNATIONAL CENTRE FOR THEORETICAL PHYSICS

Seventh Workshop
“Non-Linear Dynamics and Earthquake Prediction”
29 September to 12 October 2003

ON THE FORWARD AND BACKWARD MODELING OF MANTLE DYNAMICS

Alik T. Ismail-Zadeh

International Institute of Earthquake Prediction Theory and
Mathematical Geophysics, Russian Academy of Sciences,
Warshavskoye shosse 79-2, Moscow 113556, Russia.
E-mail: aismail@mitp.ru

Now at: Geophysical Institute, University of Karlsruhe,
Hertzsrt. 16, Karlsruhe 76187, Germany.
E-mail: Alik.Ismail-Zadeh@gpi.uni-karlsruhe.de

MIRAMARE-TRIESTE

September 2003

Numerical approach to 3D forward modeling of slow viscous flow

Igor A. Tsepelev [a,*], Alexander I. Korotkii [a], Alik T. Ismail-Zadeh [b,c]

[a] *Institute of Mathematics and Mechanics, Ural Branch, Russian Academy of Sciences, S. Kovalevskoy ul. 16, Ekaterinburg 620219, Russia*

[b] *Geophysical Institute, University of Karlsruhe, Hertzstr. 16, Karlsruhe 76187, Germany*

[c] *International Institute of Earthquake Prediction Theory and Mathematical Geophysics, Russian Academy of Sciences, Warshavskoye sh. 79-2, Moscow 113556, Russia*

Abstract

We present a numerical approach to model three-dimensional thermal convection in a viscous fluid with infinite Prandtl number and temperature-dependent density and temperature–pressure-dependent viscosity. To compute the viscous flow, we apply an Eulerian FEM (with tricubic-spline basis functions) to the Stokes equations presented in terms of a two-component vector velocity potential. The advection equations for density and viscosity are solved by the method of characteristics, and the heat equation is solved by a FDM. Numerical algorithms and code are developed to be implemented on parallel computers with a distributed memory.

Keywords: Thermal convection; Eulerian FEM; Galerkin-spline approach; Two-component vector potential

1. Introduction

Many deformational processes in the earth's crust and mantle can be described by a slow viscous flow [1–3]. Three-dimensional numerical models of the processes provide a basis for realistic simulations, but entail high computational complexity, which can be dealt with only on high-performance computers. Therefore, solution of three-dimensional problems must rely on highly efficient computational methods. Moreover, their numerical implementation frequently requires special procedures consistent with the architecture of the computer employed.

In geophysical problems, three-dimensional simulations of thermally driven convection in a rectangular domain have been performed both for constant viscosity (e.g., [4–6]) and for variable viscosity (e.g., [7–11]). The numerical simulations were based on the use of finite-difference, spectral, and multigrid methods. In this paper we present a numerical approach for solving 3D thermal convection problem using FEM, FDM, and the method of characteristics. Numerical code is developed using MPI to be employed on parallel supercomputers (IBM SP2, MPS-100/MPS-1000) with a distributed memory.

* Corresponding author. Tel.: +7 (3432) 742631;
E-mail: tsepelev@imm.uran.ru

Computational Fluid and Solid Mechanics 2003
K.J. Bathe (Editor)

2. Mathematical statement of the problem

In a spatial domain $\Omega = (0,l_1)\times(0,l_2)\times(0,l_3)$ we consider an inhomogeneous viscous incompressible flow at infinite Prandtl number in the presence of gravity and vertical temperature gradient. In Cartesian coordinates, the slow flow is described by the Stokes, incompressibility, heat, state, rheology, and advection equations:

$$-\mathrm{La}\cdot\nabla p + \mathrm{div}(\mu e_{ij}) - \mathrm{La}\cdot\rho\mathbf{e}_3, \tag{1}$$

$$\mathrm{div}\,\mathbf{u} = 0, \tag{2}$$

$$\frac{\partial(\rho_* T)}{\partial t} + \langle \mathbf{u}, \nabla(\rho_* T)\rangle = \Delta T + \mathrm{Di}\cdot\mu\Phi, \tag{3}$$

$$\rho(t,x) = \rho_*(t,x)(1-\alpha T_0\big(T(t,x)-1)\big), \tag{4}$$

$$\mu(t,x) = \mu_*(t,x)\exp\left(\frac{E_0+\rho_* x_3 p_0 V_0}{RTT_0} - \frac{E_0+p_0V_0}{RT_0}\right), \tag{5}$$

$$\frac{\partial\rho_*}{\partial t} + \langle\nabla\rho_*\mathbf{u}\rangle = 0, \qquad \frac{\partial\mu_*}{\partial t} + \langle\nabla\mu_*,\mathbf{u}\rangle = 0. \tag{6}$$

Eqs. (1)–(6) contain the following variables and parameters: time t; a spatial variable $\mathbf{x} = (x_1,x_2,x_3)$; velocity vector $\mathbf{u} = (u_1(t,x),u_2(t,x),u_3(t,x))$; pressure $p = p(t,x)$; strain rate tensor e_{ij}; absolute temperature $T = T(t,x)$; density $\rho = \rho(t,x)$; viscosity $\mu = \mu(t,x)$; thermally unperturbed density $\rho_* = \rho_*(t,x)$; thermally unperturbed viscosity $\mu_* = \mu_*(t,x)$; acceleration due to gravity g; universal gas constant R; unit vector $\mathbf{e}_3 = (0,0,1)$; coefficient of thermal expansion α; activation energy E_0; activation volume V_0; a dissipation function $\Phi = \Phi(t,x)$ representing the rate of heat production due to an internal friction; $\mathrm{La} = \rho_0 g l_0^3/(\mu_0\kappa)$; $\mathrm{Di} = \mu_0\kappa/(c\rho_0 T_0 l_0^2)$; specific heat c; thermal diffusivity κ; and reference density ρ_0, length l_0, viscosity μ_0, pressure p_0, and temperature T_0. To eliminate the incompressibility condition (Eq. 2) and pressure p from Eq. (1), we define the vector potential $\psi = (\psi_1, \psi_2, \psi_3)$ by the relation $\mathbf{u} = \mathrm{curl}\psi$ and apply the curl operator to Eq. (1).

At the boundary Γ of Ω we set impenetrability conditions with either perfect slip or no-slip conditions. For the temperature on the vertical faces on Ω we set zero heat flux conditions (as in a Neumann problem). On the top and bottom faces of Ω a specific temperature is prescribed (as in a Dirichlet problem). At the initial time temperature, density, and viscosity are given.

Equations (1–6) in terms of vector potential combined with the boundary and initial conditions determine (not uniquely) the unknown functions ψ_1, ψ_2, and ψ_3, whereas the unknown functions T, ρ_*, and μ_*, (and, therefore, ρ and μ) are uniquely determined within Ω at any $t \geq 0$. For our purposes, any potential found by solving the equations above is suitable, because the same velocity field is obtained.

3. Numerical methodology

To apply a finite element method, we replace Eq. (1) by the following variational equation

$$\int_\Omega \mu\big(2e_{11}\xi_{11} + 2e_{22}\xi_{22} + 2e_{33}\xi_{33} + e_{12}\xi_{12} + e_{13}\xi_{13} + e_{23}\xi_{23}\big)\mathrm{d}x = -\mathrm{La}\int_\Omega \rho\omega_3\,\mathrm{d}x, \tag{7}$$

for any arbitrary admissible function $\boldsymbol{\omega} = (\omega_1, \omega_2, \omega_3)$, where the expressions for ξ_{ij} in terms of $\boldsymbol{\omega}$ are identical to the expressions for e_{ij} in terms of $\boldsymbol{\psi}$; and function $\boldsymbol{\omega}$ satisfies the conditions set for the vector potential $\boldsymbol{\psi}$.

Ismail-Zadeh et al. [12] showed that the three-component vector potential can be reduced to a two-component representation for a wide class of problems, so that $\psi_3 = 0$ in the required vector velocity potential ψ. If viscosity of the fluid is only depth dependent, that is $\mu = \mu(t, x_3)$, the two-component representation can be replaced by one-component potential $\boldsymbol{\psi} = (\partial\varphi/\partial x_2, -\partial\varphi/\partial x_1, 0)$, where $\varphi = \varphi(t,x)$ is a scalar function satisfying appropriate boundary conditions.

Therefore, the problem is reduced to computing the functions $\boldsymbol{\psi}(t,x)$, $T = T(t,x)$, $\rho(t,x)$, and $\mu(t,x)$ that satisfy Eqs. (3–7) in Ω at $t \geq 0$ and the boundary and initial conditions formulated above.

Vector potential $\boldsymbol{\psi}$, the thermally unperturbed density ρ_* and viscosity μ_* are found by applying an Eulerian FEM with basis functions of a special form. The construction of the basis functions and the implementation of the finite element method were described in detail by Ismail-Zadeh et al. [13]. The vector potential is approximated by a linear combination of tricubic basis functions expressed as products of cubic splines. Density and viscosity are approximated at three times finer grid by linear combinations of trilinear basis functions expressed as products of linear functions.

The approximate vector potential is found for prescribed density and viscosity distributions by solving a set of linear algebraic equations with a positive definite band matrix. We solve the system by the conjugate gradient or Seidel iteration method [14]. Approximations of the thermally unperturbed density and viscosity for a prescribed velocity distribution are computed by the method of characteristics (see [13]). Temperature $T = T(t,x)$ is approximated by finite-differences and computed by the implicit alternating-direction method [15]. At each iteration timestep, a large set of linear algebraic equations is solved, and a number of independent modules are organized for solving these equations on parallel supercomputers with a distributed memory.

The numerical algorithm consists of the following basic steps: (i) a set of linear algebraic equations is solved for the coefficients of a decomposition of the vector velocity potential in terms of basis functions; (ii) the approximate heat equation and Eq. (6) for advection of the thermally unperturbed density ρ_* and viscosity μ_* are then solved; and (iii) updated density and viscosity are determined from Eqs. (4) and (5), respectively.

4. Conclusions

In summary we derive the following conclusions. A numerical method was developed to solve simultaneously the Stokes equations, heat equation, and advection equations, where the fluid density and viscosity are temperature- and temperature–pressure-dependent, respectively.

A computational cost is greatly reduced by an introduction of the two-component (or even one-component in some cases) representation of the vector velocity potential.

The use of tricubic splines as basis functions in an approximation of the vector velocity potential allows to obtain numerical results of high accuracy.

Numerical experiments have showed an efficiency of the numerical algorithm and parallelized code developed.

Acknowledgments

This research was supported by the ISTC (1293-99) and RFBR (02-01-00354). A.T.I-Z was supported by the Alexander von Humboldt Foundation.

References

[1] Turcotte DL, Schubert G. Geodynamics, 2nd edition. Cambridge: Cambridge University Press, 2002.
[2] Lliboutry LA. Very Slow Flows of Solids. Basics of Modeling in Geodynamics and Glaciology. Dordrecht: Martinus Nijhoff Publishers, 1987.
[3] Schubert G, Turcotte DL, Olson P. Mantle Convection in the Earth and Planets. Cambridge: Cambridge University Press, 2001.
[4] Cserepes L, Rabinowicz M, Rosemberg-Borot C. Three-dimensional convection in a two-layer mantle. J Geophys Res 1988;93:12009–12025.
[5] Houseman G. The dependence of convection planform on mode of heating. Nature 1988;332: 346–349.
[6] Travis B, Olson P, Schubert G. The transition from two-dimensional to three-dimensional planforms in infinite-Prandtl-number thermal convection. J Fluid Mech 1990; 216:71–91.
[7] Frick H, Busse FH, Clever RM. Steady three-dimensional convection at high Prandtl number. J Fluid Mech 1983; 127:141–153.
[8] Christensen U, Harder H. 3-D convection with variable viscosity. Geophys J Int 1991;104:213–226.
[9] Ogawa M, Schubert G, Zebib A. Numerical simulation of three-dimensional thermal convection in a fluid with strongly temperature-dependent viscosity. J Fluid Mech 1991;233:299–328.
[10] Tackley PJ. Effects of strongly temperature-dependent viscosity on time-dependent, three-dimensional models of mantle convection. Geophys Res Lett 199;20:2187–2190.
[11] Trompert RA, Hansen U. The application of a finite volume multigrid method to three-dimensional flow problems in a highly viscous fluid with a variable viscosity. Geophys Astrophys Fluid Dyn 1996;83:261–291.
[12] Ismail–Zadeh AT, Korotkii AI, Naimark BM, Tsepelev IA. Numerical modelling of three–dimensional viscous flow under gravity and thermal effects. Comput Math Math Phys 2001;41:1428–1444.
[13] Ismail-Zadeh AT, Korotkii AI, Naimark BM, Suetov AP, Tsepelev IA. Implementation of a three-dimensional hydrodynamic model for evolution of sedimentary basins. Comput Math Math Phys 1998;38:1138–1151.
[14] Golub G, van Loan C. Matrix Computations, 3rd ed. Baltimore: John Hopkins University Press, 1996.
[15] Marchuk GI. Numerical Methods and Applications. Boca Raton: CRC Press, 1994.

Numerical approach to solving problems of slow viscous flow backwards in time

A.T. Ismail-Zadeh [a,b,*], A.I. Korotkii [c], I.A. Tsepelev [c]

[a] *Geophysical Institute, University of Karlsruhe, Hertzstr. 16, Karlsruhe 76187, Germany*
[b] *International Institute of Earthquake Prediction Theory and Mathematical Geophysics, Russian Academy of Sciences, Warshavskoye sh. 79-2, Moscow 113556, Russia*
[c] *Institute of Mathematics and Mechanics, Ural Branch, Russian Academy of Sciences, S. Kovalevskoy ul. 16, Ekaterinburg 620219, Russia*

Abstract

We present an approach to three-dimensional numerical solutions of gravity advection (Rayleigh–Taylor) and thermal convection (Rayleigh–Benard) problems. The inverse problem of gravity advection is solved numerically by replacing positive timesteps with negative ones. The inverse problem of thermal convection is ill-posed problem, and we suggest a variational approach to solve the problem. We test the numerical methodology on restoration models of diapirs and a thermal plume. The numerical approach can be used to reconstruct evolutions of salt and mud diapirs, mantle plumes and lithospheric slabs.

Keywords: Rayleigh–Taylor instability; Rayleigh–Benard instability; Ill-posed problem; Backward heat equation; Optimization methods

1. Introduction

A restoration of geological structures means a finding of a spatial distribution of physical variables (e.g., velocity, density, viscosity, temperature) in the geological past using some information about their present-day distributions. Hence to restore the evolution of geo-structures, it is necessary to solve a system of partial differential equations backwards in time. The principal goal of the study was to develop stable numerical algorithms to simulate the inverse problems of gravity advection and thermal convection.

2. Mathematical statement of the problems

2.1. Problem 1. Gravity advection

In 3D model domain $\Omega_1 = [0,3h] \times [0,3h] \times [0,h]$ we consider a slow flow of viscous heterogeneous incompressible fluid due to gravity. The flow is governed by the momentum, advection, and continuity equations. The dimensionless equations take the following form [1]:

$$\nabla P = \operatorname{div}(\mu e_{ij}) + g\rho\vec{e}_3, \quad (1)$$

$$\partial\rho/\partial t + \langle\vec{u}, \nabla\rho\rangle = 0, \quad \partial\mu/\partial t + \langle\vec{u}, \nabla\mu\rangle = 0, \quad t \in [0, \vartheta], \quad (2)$$

$$\operatorname{div}\vec{u} = 0, \quad t \in [0, \vartheta], \quad x \in \Omega_1. \quad (3)$$

2.2. Problem 2. Thermal convection

In 3D model domain $\Omega_2 = [0,2h] \times [0,2h] \times [0,h]$ we consider a slow thermoconvective flow of heterogeneous incompressible fluid at the infinite Prandtl number with a temperature-dependent viscosity. The flow is described by heat, momentum, and continuity equations. In the Boussinesq approximation these dimensionless equations take the following form [1]:

$$\partial T/\partial t + \langle\vec{u}, \nabla T\rangle = \nabla^2 T, \quad t \in (0, \vartheta], \quad x \in \Omega_2, \quad (4)$$

$$\nabla P = \operatorname{div}(\mu e_{ij}) + \mathrm{Ra}\, T\vec{e}_3, \quad e_{ij} = \partial u_i/\partial x_j + \partial u_j/\partial x_i,$$
$$\vec{e}_3 = (0,0,1), \quad (5)$$

$$\operatorname{div}\vec{u} = 0 \quad t \in [0, \vartheta], \quad x \in \Omega_2. \quad (6)$$

Here T, t, $\vec{u}$, P, ρ, and μ are temperature, time, velocity vector, pressure, density and viscosity, respectively. The

* Corresponding author. Tel.: +49 721-6084621; Fax: +49 721-71173; E-mail: alik.ismail-zadeh@gpi.uni-karlsruhe.de

Computational Fluid and Solid Mechanics 2003
K.J. Bathe (Editor)

Rayleigh number is defined as $\mathrm{Ra} = \alpha g \rho_0 \delta T h^3 / \mu_0 \kappa$ where α is the thermal expansivity; g is the acceleration due to gravity; ρ_0 and μ_0 are the reference density and viscosity, respectively; δT is the temperature contrast between the upper and lower boundary of the model domain; and κ is the thermal diffusivity. In Eqs. (4)–(6) length, temperature, and time are normalized by h, δT, and h^2/κ, respectively.

At the boundary of the model domain (Problems 1 and 2) we set the impenetrability condition with perfect slip conditions: $\langle \vec{u}, \vec{n} \rangle = 0$, $\langle \nabla \vec{u}_{tg}, \vec{n} \rangle = 0$, where $\vec{n}$ is the normal vector and u_{tg} is the tangential component of velocity. In Problem 2 we assume the heat flux through the vertical boundaries of the box to be zero: $\langle \vec{n}, \nabla T \rangle = 0$. The upper and lower boundaries are isothermal surfaces, and hence $T = 0$ and $T = 1$ at the boundaries respectively. To solve the direct (forward in time) and inverse (backward in time) problems of gravity advection (Problem 1), we assume the density and viscosity to be known at the initial time $t = 0$ and at the final (in terms of the direct problem) time $t = \vartheta$, respectively. To solve the direct and inverse problems of thermal convection (Problem 2), we assume the temperature to be known at the initial time $t = 0$ and at the final time $t = \vartheta$, respectively.

Thus, the direct (or inverse) problem of gravity advection is to determine functions $\vec{u} = \vec{u}(t,x)$, $P = P(t,x)$, $\rho = \rho(t,x)$, and $\mu = \mu(t,x)$ satisfying (1)–(3) at $t \geq 0$ (or $t \leq \vartheta$), prescribed boundary conditions, and the initial condition for the direct problem and the final condition for the inverse problem. The direct (or inverse) problem of the thermal convection is to determine functions $\vec{u} = \vec{u}(t,x)$, $P = P(t,x)$, and $T = T(t,x)$ satisfying (4)–(6) at $t \geq 0$ (or $t \leq \vartheta$), prescribed boundary conditions, and the initial condition for the direct problem and the final condition for the inverse problem.

3. Numerical approach

A numerical solution to Stokes equations (1) and (5) is based on an introduction of a two-component vector velocity potential and on the application of the Eulerian FEM with a tricubic-spline basis for computing the potential [2]. Such a procedure results in a set of linear algebraic equations with a symmetric positive-defined banded matrix. We solve the set of the equations by the conjugate gradient method. The numerical algorithm was designed to be implemented on parallel computers. Temperature entering in the heat equation (4) is approximated by finite differences and found by the alternating direction method [3].

Equations (2) have characteristics described by the system of ordinary differential equations

$$\mathrm{d}x/\mathrm{d}t = \vec{u}(t, x(t)). \tag{7}$$

Along the characteristics the density and viscosity are constant $\rho(t, x(t)) = \rho_*(x(0))$, $\mu(t, x(t)) = \mu_*(x(0))$, where ρ_* and μ_* are the initial density and viscosity. The characteristics are computed with the Euler or Runge–Kutta methods. If we replace the positive time by the negative in (7), we have the same form of characteristics for inverse velocity field [4]. It should be noted that conjugated problems to (2) have the same form for inverse velocity field too.

It is known that an inverse problem of thermal convection is ill-posed, because the inverse operator of the heat equation is non-bounded. As a result, small errors in computations (or in estimations of present-day temperature field) will result in large errors in a solution of the problem. The method suggested here for solving the inverse problem of thermal convection is included into a class of variational methods.

We consider the following objective functional $J(\varphi) = \|T(\vartheta, \cdot; \varphi) - \chi(\cdot)\|^2$, where $T(\vartheta, \cdot; \varphi)$ is the solution of the thermal boundary problem (4) at the final time ϑ, which corresponds to some (unknown as yet) initial temperature distribution $\varphi(\cdot)$; $\chi(\cdot) = T(\vartheta, \cdot; T_0)$ is the known temperature distribution at the final time, which corresponds the initial temperature $T_0(\cdot)$, and $\|\cdot\|$ is the norm in space $L^2(\Omega)$. The functional has its unique global minimum at value $\varphi \equiv T_0$ and $J(T_0) \equiv 0$, $\nabla J(T_0) \equiv 0$. The uniqueness of the functional's minimum follows from the uniqueness of the solution of the relevant boundary value problem for the heat equation [5]. Therefore, we seek the global minimum of the functional with respect to φ. To find a minimum of the functional we employ the gradient method [6] $(k = 0, 1, \ldots, n, \ldots)$

$$\begin{aligned} &\varphi_{k+1} = \varphi_k - \beta_k \nabla J(\varphi_k), \\ &\beta_k = \min\{1/(k+1), J(\varphi_k)/\|\nabla J(\varphi_k)\|^2\}, \qquad \varphi_0 = 0. \end{aligned} \tag{8}$$

We found ∇J as a solution to the boundary problem conjugated to (4) at the initial time:

$$\partial Z/\partial \tau - \langle \vec{u}, \nabla Z \rangle = \nabla^2 Z, \qquad \tau = -t \in [0, \vartheta), \tag{9}$$

$$Z(\vartheta, x) = 2(T(\vartheta, x; \varphi) - \chi(x)),$$

with uniform boundary conditions. The iterative solution algorithm for the backward heat equation is based on the following three steps $(k = 0, 1, \ldots, n, \ldots)$: (i) to solve the heat equation (4) with appropriate boundary conditions and initial condition $T = \varphi_k$ at time interval $[0, \vartheta]$ in order to find $T(\theta, \cdot; \varphi_k)$; (ii) to solve problem (9) backwards in time, that is, to determine gradient $\nabla J(\varphi_k)$ of functional; and (iii) to determine β_k and then to find φ_{k+1} from (8). Computations are terminated, when condition $J(\tilde{\varphi}_k) < \varepsilon$ is true, and $\tilde{\varphi}_k$ is then considered to be an approximate solution to the backward heat equation. The parameter ε depends on an accuracy of finite difference approximations for the heat equation. Thus, the solution to the backward heat equation with the appropriate boundary and initial conditions was reduced to solutions of series of forward problems, which are known to be well-posed.

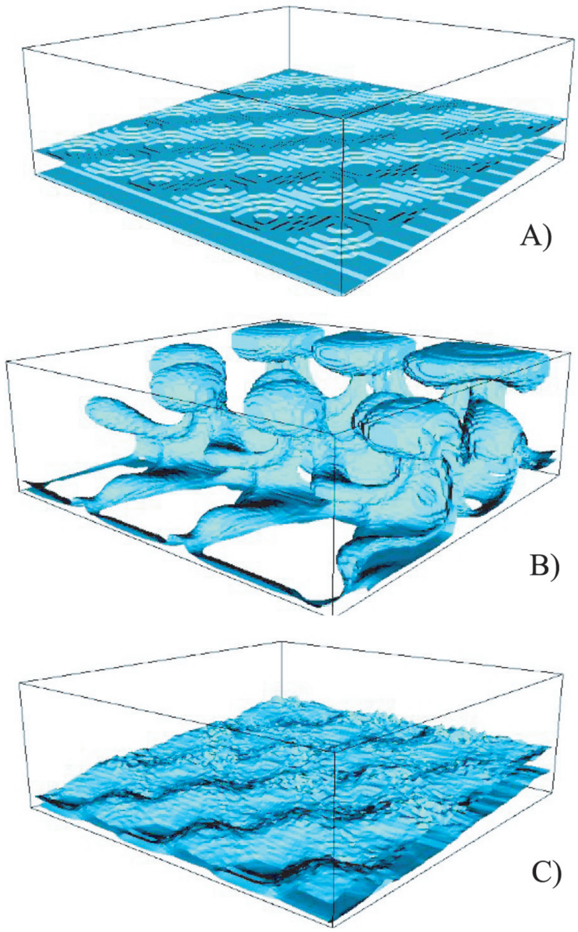

Fig. 1. Gravity advection problem. Forward and backward modeling of a diapir evolution.

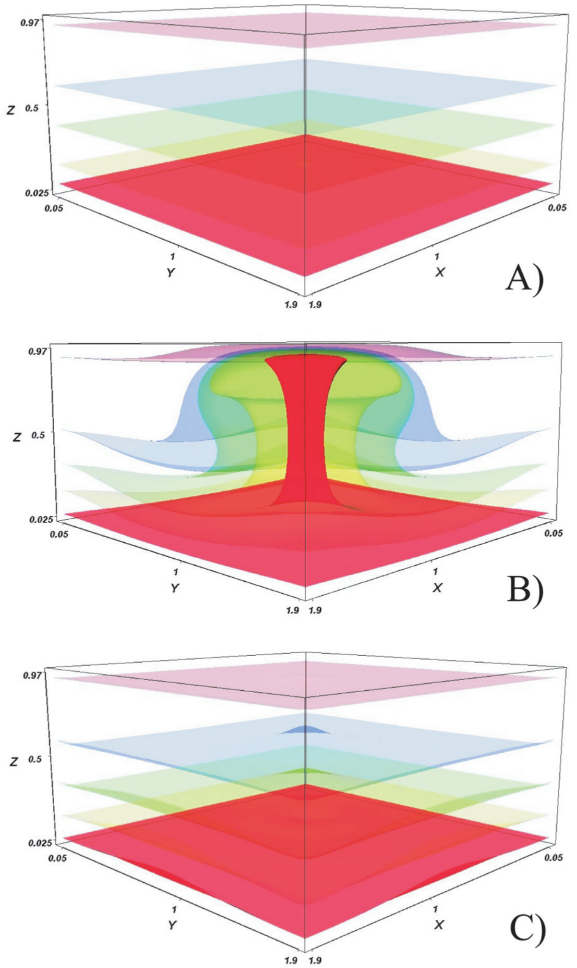

Fig. 2. Thermal convection problem. Forward and backward modeling of a thermal plume evolution.

4. Results

To model the problem of gravity advection backwards in time we consider a three-layered structure of viscous fluid filling the model domain. The viscosities and densities are $\mu = 1.0$ and $\rho = 0.85$ for the middle layer, $\mu = 100.0$ and $\rho = 1.0$ for the lower and upper layers, respectively. Fig. 1 illustrates interfaces between the layers at the initial (a) and final (b) times for the direct problem, and restorations of the layers (c) from their positions illustrated in (b).

To model the backward thermal convection, we consider that $T_0 = 1 - x_3/h$, $\mathrm{Ra} \approx 9 \times 10^4$, $\mu(T) = \exp(Q/(T+G) - Q/(0.5+G))$, $Q = 225/\ln(r) - 0.25\ln(r)$, $G = 15/\ln(r) - 0.5$, and $r = 20$ is the viscosity ratio between the upper and lower boundaries of the model domain [7]. In the forward model we prescribe a small thermal perturbation at the initial time in $x = (0.5, 0.5, 0.1)$ to generate instability and to evolve a thermal plume. We divide model box into $32 \times 32 \times 32$ rectangular elements to approximate vector potential and viscosity. Temperature and density were approximated on the grid $94 \times 94 \times 94$. Time step $\Delta t = \mathrm{d}x/u_{\max}$, $u_{\max} = \max_{\Omega} |u|$, $\mathrm{d}x$ is diameter of the grid. Fig. 2 presents the initial positions of the isotherms for the direct problem of the thermal convection (a), the final position of the isotherms (b), and their restorations (c).

5. Conclusion

We suggested new numerical approaches to solving the inverse problems of gravity advection and thermal convection. In the case of thermal convection we reduce the ill-posed backward problem to iterative solving well-posed direct and conjugated problems for the heat equation. The solution algorithms are stable to small computational errors and able to restore viscous flow, density, and temperature. Our approach allows using parallelized computer codes developed for simulations of forward problems. The suggested methodology opens a new possibility in problems of restorations of geological structures.

Acknowledgements

The research was supported by the ISTC (99-1293) and RFBR (02-01-00354). A financial support from the A. von Humboldt Foundation to A.T. I.-Z. is gratefully acknowledged.

References

[1] Chandrasekhar S. Hydrodynamic and hydromagnetic stability. Oxford: University Press, 1961.

[2] Ismail-Zadeh AT, Korotkii AI, Naimark BM, Tsepelev IA. Numerical simulation of three-dimensional viscous flows with gravitational and thermal effects. Comput Math Mathem Phys 2001;41:1399–1415.

[3] Marchuk GI. Numerical methods and applications. Boca Raton: CRC Press, 1994.

[4] Ismail-Zadeh AT, Talbot CJ, Volozh YA. Dynamic restoration of profiles across diapiric salt structures: numerical approach and its applications. Tectonophysics 2001;337:23–38.

[5] Tikhonov AN, Samarskii AA. Equations of mathematical physics. New York: Dover Publications, 1990.

[6] Vasiliev FP. Metody optimizatsii. Moscow: Faktorial Press, 2002.

[7] Busse FH, et al. 3D convection at infinite Prandtl number in Cartesian geometry — a benchmark comparison. Geophys Astrophys Fluid Dynamics 1993;75:39–59.

Inverse Problem of Thermal Convection: Numerical Approach and Application to Mantle Plume Restoration

Alik Ismail-Zadeh[123], Gerald Schubert[3], Igor Tsepelev[4] and Alexander Korotkii[4]

[1]International Institute of Earthquake Prediction Theory and Mathematical Geophysics, Russian Academy of Sciences, Moscow, Russia

[2]Geophysical Institute, University of Karlsruhe, Germany

[3]Department of Earth & Space Sciences, Institute of Geophysics and Planetary Physics, University of California, Los Angeles, USA

[4]Institute of Mathematics and Mechanics, Ural Branch, Russian Academy of Sciences, Yekaterinburg, Russia

Short title: INVERSE PROBLEM OF MANTLE CONVECTION

Abstract.

Modern seismic tomographic images of the Earth's interior facilitate the inference of the complex trajectories of present-day convective flow in the upper mantle. Quantitative reconstruction of both the observed mantle structure and temperature field backwards in time requires a numerical tool for solving the inverse problem of thermal convection at infinite Prandtl number. In this paper we present a variational approach to three-dimensional numerical restoration of thermoconvective mantle flow with temperature-dependent viscosity. This approach is based on a search for the mantle temperature and flow in the geological past by minimizing differences between present-day mantle temperature derived from seismic velocities (or their anomalies) and that predicted by forward models of mantle flow for an initial temperature guess. The past mantle temperatures so obtained can be employed as constraints on forward models of mantle dynamics. To demonstrate the applicability of this technique, we restore numerically a fluid dynamic model of the evolution of upper mantle plumes and show that the initial shape of the plumes can be accurately reconstructed. We then model the evolution of the plumes forward in time (plume upbuilding) starting from the restored state to the state they were before the restoration and demonstrate the high accuracy of the model predictions. We also show that the neglect of thermal diffusion in the backward modeling of thermal plumes (in order to simplify the numerical procedure) results in erroneous restorations of the plumes.

Introduction

The reconstruction of mantle plumes and lithospheric slabs to earlier stages of their evolution is a major challenge in geodynamics. High-resolution seismic tomographic studies open possibilities for detailed observations of present-day mantle structures [e.g., *Grand et al.,* 1997; *van der Voo et al.,* 1999; *Ritsema and Allen,* 2003] and for derivations of mantle temperature from seismic velocities or velocity anomalies [e.g., *Sobolev et al.,* 1996; *Goes et al.,* 2000]. An accurate reconstruction would allow the test of geodynamic models by simulating the evolution of plumes or slabs starting from the restored state and comparing the derived forward state to observations.

For clarity of subsequent discussion, we introduce a few mathematical definitions used in the paper. A mathematical model for a geophysical problem has to be *well-posed* in the sense that it has to have the properties of existence, uniqueness, and stability of a solution to the problem [*Hadamard,* 1923]. Problems for which at least one of these properties does not hold are called *ill-posed*. The requirement of stability is the most important one. If a problem lacks the property of stability then its solution is almost impossible to compute because numerical computations are polluted by unavoidable errors. If the solution of a problem does not depend continuously on the initial data, then, in general, the computed solution may have nothing to do with the true solution.

The inverse problem of thermal convection in the mantle is an ill-posed problem, since the backward heat problem, describing both heat advection and diffusion through the mantle backwards in time, possesses the properties of ill-posedness [*Kirsch,* 1996].

In particular, the solution to the problem does not depend continuously on the initial data. This means that small changes in the present-day temperature field may result in large changes of predicted mantle temperatures in the past (see Appendix 1 for an explanation of this statement in the case of the 1-D diffusion equation).

If heat diffusion is neglected, the solution of the advection equation backwards in time does not present computational difficulties. A numerical approach to the solution of the inverse problem of the Rayleigh-Taylor (gravitational) instability was proposed by *Ismail-Zadeh* [1999] and was developed later for a dynamic restoration of plume (diapiric) structures to their earlier stages [*Ismail-Zadeh et al.*, 2001a]. *Kaus and Podladchikov* [2001] and *Korotkii et al.* [2002] applied the approach to study 3D Rayleigh-Taylor overturns forward and backward in time. Both direct (forward in time) and inverse (backward in time) problems of the gravitational advection are well-posed. This is because the time-dependent advection equation (for density or temperature) has the same form of characteristics for the direct and inverse velocity field (the vector velocity reverses its direction, when time is reversed). Therefore, numerical algorithms used to solve the direct problem of the gravitational instability of the geological structures can also be used in studies of the inverse problems by replacing positive timesteps with negative ones.

Steinberger and O'Connell [1997, 1998] and *Conrad and Gurnis* [2003] modeled the mantle flow backwards in time from present-day mantle density heterogeneities inferred from seismic observations. However, they ignored thermal diffusion in the mantle (and hence the respective term in the heat equation) and employed the advection equation in the modeling. We demonstrate that this approach (neglect of heat diffusion in backward modeling) is not valid.

There is sizeable literature on the numerical solution of the backward heat equation (e.g., *Buzbee and Carasso* [1973], *Colton* [1979], *Elden* [1982], *Ames and Epperson* [1997], *Lu* [1997], *Moszynski* [2001]; see also *Tikhonov and Arsenin* [1977] and *Kirsch* [1996] for additional references). These methods are based on a regularization of the numerical solution. *Bunge et al.* [2003] and *Ismail-Zadeh et al.* [2003a,b] have independently developed variational approaches for solving the inverse problem of mantle convection. The major differences between the two approaches are that *Bunge et al.* [2003] applied the variational method to a set of equations describing mantle convection, whereas *Ismail-Zadeh et al.* [2003a] applied the variational method to the heat equation, because time enters only into this equation and the backward heat problem is ill-posed. *Ismail-Zadeh et al.* [2003a] determine the temperature in the geological past and then the convective backward flow from the Stokes and continuity equations. (We will discuss other differences between these two approaches to solving the inverse problem of mantle convection later in the paper.)

In section 1 we present a mathematical statement of the three-dimensional direct and inverse problems of thermal convection with temperature-dependent viscosity. In section 2 we describe the variational approach to search for mantle temperature in the geological past based on estimations of its present-day temperature. The approach is based on reducing the problem to minimization of the objective functional describing the difference between the present-day mantle temperature and that predicted by forward models of mantle flow for an initial temperature guess. The optimum solution to the minimization problem is provided by iteratively solving coupled direct and conjugate (adjoint) problems for the heat equation. The variational approach to solving the backward heat problem has been known in applied mathematics and geophysics (meteorology and oceanology), but so far has not been used in studies of mantle thermoconvective flow. In section 3 we describe numerical techniques used in solving the inverse problem of mantle convection. We demonstrate the applicability of the numerical approach to restoration of mantle plumes and show the effect of heat diffusion on results of the backward modeling in sect. 4. We discuss the physical and mathematical meaning of the time-reversible processes in sect. 5 and present conclusions in sect. 6.

1. Mathematical Statement of the Problem

We assume that the mantle behaves as a Newtonian fluid at geological time scales and consider the slow thermoconvective flow of a heterogeneous incompressible fluid at infinite Prandtl number with a temperature-dependent viscosity in a three-dimensional rectangular domain $\Omega = (0, x_1 = l_1) \times (0, x_2 = l_2) \times (0, x_3 = l_3 = h)$ heated from below; $x = (x_1, x_2, x_3)$ are the spatial coordinates; the x_3-axis is vertical and positive upward. Thermoconvective flow is described by the heat, momentum (Stokes), and continuity equations. In the Boussinesq approximation these dimensionless equations take the form [*Chandrasekhar,* 1961]:

$$\partial T/\partial t + \mathbf{u} \cdot \bigtriangledown T - \bigtriangledown^2 T = 0, \tag{1}$$

$$-\bigtriangledown P + \bigtriangledown \cdot [\mu(T)(\bigtriangledown \mathbf{u} + (\bigtriangledown \mathbf{u})^{Tr})] + Ra\, T\, \mathbf{e} = 0, \tag{2}$$

$$\bigtriangledown \cdot \mathbf{u} = 0, \tag{3}$$

for $x \in \Omega$ and $t \in (\vartheta_1, \vartheta_2)$, where T, $\mathbf{u}$, P, μ, and t are temperature, velocity, pressure, viscosity, and time respectively; superscript ^{Tr} means transpose; and $\mathbf{e} = (0, 0, 1)$ is the unit vector. The Rayleigh number is defined as $Ra = \alpha g \rho_0 \bigtriangleup T h^3/\mu_0 \kappa$ where α is the thermal expansivity; g is the acceleration due to gravity; ρ_0 and μ_0 are the reference typical density and viscosity, respectively; $\bigtriangleup T$ is the temperature contrast between the lower and upper boundaries of the model domain; and κ is the thermal diffusivity. In Eqs. (1)-(3) length, temperature, and time are normalized by h, $\bigtriangleup T$, and h^2/κ, respectively. We do not consider the chemical convection in the mantle. The formulation of the inverse problem of thermo-chemical convection and the numerical approach to the solution of the problem are described by *Ismail-Zadeh et al.* [2003a].

At the boundary Γ of the model domain Ω we set the impenetrability and perfect slip conditions: $\mathbf{n} \cdot \bigtriangledown \mathbf{u}_{tg} = 0$ and $\mathbf{n} \cdot \mathbf{u} = 0$, where $\mathbf{n}$ is the outer normal vector and $\mathbf{u}_{tg}$ is the tangential component of velocity. We assume the heat flux through the vertical boundaries of Ω to be zero: $\mathbf{n} \cdot \bigtriangledown T = 0$. The upper and lower boundaries are assumed to be isothermal surfaces, and hence $T = T_u$ at $x_3 = h$, $T = T_l$ at $x_3 = 0$, where T_u and T_l are constant, and $\Delta T = T_l - T_u > 0$. To solve the direct and inverse problems of thermal convection, we assume that the temperature is known at the initial time $t = \vartheta_1$ and at the final (in terms of the direct problem) time $t = \vartheta_2$, respectively.

Thus, the direct (or inverse) problem of the thermal convection is to determine velocity, $\mathbf{u} = \mathbf{u}(t, x)$, pressure, $P = P(t, x)$, and temperature, $T = T(t, x)$, satisfying Eqs. (1)-(3) at $t \geq \vartheta_1$ (or $t \leq \vartheta_2$), the prescribed boundary conditions, and the temperature condition at $t = \vartheta_1$ (or $t = \vartheta_2$).

2. Variational Approach to Solving the Backward Heat Problem

In this section we present a variational approach to an approximate solution to the backward heat problem. Consider the following objective (quadratic) functional

$$J(\varphi) = \|T(\vartheta_2, \cdot\,; \varphi) - \chi(\cdot)\|^2 = \int_\Omega |T(\vartheta_2, x; \varphi) - \chi(x)|^2 dx, \tag{4}$$

where $T(\vartheta_2, x; \varphi)$ is the solution of the forward heat equation (1) with the appropriate boundary and initial conditions at final time ϑ_2, which corresponds to some (unknown as yet) initial temperature distribution $\varphi = \varphi(x)$; $\chi(x) = T(\vartheta_2, x; T_0)$ is the known temperature distribution at the final time for the initial temperature $T_0 = T_0(x)$; and $\|\cdot\|$ is the norm in space $L^2(\Omega)$. We seek a minimum of the objective functional with respect to the initial temperature, φ. The functional has its unique global minimum at value $\varphi = T_0$, and $J(T_0) = 0$, $\bigtriangledown J(T_0) = 0$. The uniqueness of the global minimum of the objective functional follows from the uniqueness of the solution of the relevant boundary value problem for the heat equation and a strong convexity of the functional [*Tikhonov and Samarskii,* 1990].

To find a minimum of the objective functional we employ the gradient method

[*Vasiliev,* 2002]

$$\varphi_{k+1} = \varphi_k - \alpha_k \bigtriangledown J(\varphi_k), \quad \varphi_0 = T_*, \quad k = 0, 1, 2, ... , \tag{5}$$

$$\alpha_k = \min\{1/(k+1); J(\varphi_k)/\| \bigtriangledown J(\varphi_k)\|\}, \tag{6}$$

where T_* is an initial temperature guess. It can be shown that the gradient of functional J is represented as $\bigtriangledown J(\varphi) = \Psi(\vartheta_1, \cdot\,)$ (see Appendix 2), where Ψ is the solution to the following boundary problem conjugated (adjoint) to the respective boundary problem for Eq. (1):

$$\begin{aligned} &\partial\Psi/\partial t + \mathbf{u} \cdot \bigtriangledown\Psi + \bigtriangledown^2\Psi = 0, && x \in \Omega, \quad t \in (\vartheta_1, \vartheta_2), \\ &\sigma_1\Psi + \sigma_2 \partial\Psi/\partial\mathbf{n} = 0, && x \in \Gamma, \quad t \in (\vartheta_1, \vartheta_2), \\ &\Psi(\vartheta_2, x) = 2(T(\vartheta_2, x; \varphi) - \chi(x)), && x \in \Omega, \end{aligned} \tag{7}$$

where σ_1 and σ_2 are some smooth functions or constants satisfying the condition $\sigma_1^2 + \sigma_2^2 \neq 0$. Selecting σ_1 and σ_2 we can obtain corresponding boundary conditions. Problem (7) is ill-posed for positive timesteps and well-posed for negative timesteps.

The solution algorithm for the backward heat problem is based on the following three steps ($k = 0, 1, 2, ..., n, ...$):

(i) solve the forward heat equation (1) in the time interval $[\vartheta_1, \vartheta_2]$, $x \in \Omega$, with the boundary conditions defined and initial temperature $T(\vartheta_1, x) = \varphi_k(x)$ in order to find $T(\vartheta_2, x; \varphi_k)$;

(ii) solve problem (7) backwards in time and determine $\bigtriangledown J(\varphi_k) = \Psi(\vartheta_1, x; \varphi_k)$; and

(iii) determine α_k from (6) and then update the initial temperature, i.e., find φ_{k+1} from (5).

Computations are terminated when

$$\delta\varphi_n = J(\varphi_n) + \| \bigtriangledown J(\varphi_n)\|^2 < \varepsilon, \tag{8}$$

where ε is a small constant (in our numerical experiments we assumed $\varepsilon = 10^{-8}$). The temperature φ_n is then considered to be the approximation of the target value of the initial temperature T_0. If $\delta\varphi_n \geq \varepsilon$, we return to step (i) and make the next iteration. Numerical tests demonstrate that if the initial guess for temperature is a smooth function, than iterations converge rapidly (only 5 to 10 iterations); otherwise, the iterations converge very slowly (100 and more iterations).

Thus, the solution of the backward heat problem is reduced to solutions of series of forward problems, which are known to be well-posed [*Tikhonov and Samarskii,* 1990]. The algorithm can be used to solve the problem over any subinterval of time in $[\vartheta_1, \vartheta_2]$.

3. Numerical Approach to Solving the Inverse Problem of Mantle Convection

In this section we describe briefly the numerical methods we use in the study. See *Ismail-Zadeh et al.* [2001b] for more detail.

3.1. Numerical Method for Solving the Stokes Equation

To facilitate computations, Eqs. (2) and (3) are simplified by introducing a two-component representation of the vector velocity potential

$$\mathbf{u} = \text{curl } \vec{\psi}, \quad \vec{\psi} = (\psi_1,\ \psi_2,\ 0)\ . \tag{9}$$

We represent the vector velocity potential as a linear combination of tricubic basis splines and apply the Eulerian finite element method to Eqs. (2) and (3) with the appropriate boundary conditions. To simplify analysis, we rewrite the problem in variational form. To solve the problem numerically, the model domain Ω is discretized introducing the uniform rectangular grid

$$0 = x_i^0 < x_i^1 < ... < x_i^{n_i-1} < x_i^{n_i} = l_i, \quad i = 1, 2, 3,$$

with grid points $\Omega_{ijk} = (x_1^i, x_2^j, x_3^k)$, $0 \leq i \leq n_1$, $0 \leq j \leq n_2$, and $0 \leq k \leq n_3$. At each grid point Ω_{ijk}, we define a tricubic basis element $\omega_{ijk}^l = \omega_{ijk}^l(x_1, x_2, x_3)$, $l = 1, 2$ as the tensor product of one-dimensional cubic basis elements (*Ahlberg et al.,* 1967). The construction of bases consisting of tricubic elements ω_{ijk}^l is described by *Ismail-Zadeh et al.* [1998].

The vector potential is approximated by the combinations

$$\psi_l(t, x_1, x_2, x_3) \approx \sum_{i,j,k} \psi_{ijk}^l(t)\ \omega_{ijk}^l(x_1, x_2, x_3), \quad l = 1, 2. \tag{10}$$

Density and viscosity are approximated by using trilinear basis elements $\phi_{ijk}(x_1, x_2, x_3)$:

$$\rho(t, x_1, x_2, x_3) \approx \sum_{i,j,k} \rho_{ijk}(t)\ \phi_{ijk}(x_1, x_2, x_3),$$

$$\mu(t, x_1, x_2, x_3) \approx \sum_{i,j,k} \mu_{ijk}(t)\ \phi_{ijk}(x_1, x_2, x_3).$$

The coefficients ψ_{ijk}^l are determined at each time step by solving a set of linear algebraic equations with a symmetric positive definite band matrix. The set is solved iteratively by conjugate gradient or Gauss–Seidel methods. The relevant software was designed for implementing the codes on parallel computers. A detailed analysis of particular implementations of iterative methods for sets of linear algebraic equations is presented by *Tsepelev et al.* [1999].

3.2. Numerical Method for Solving the Heat Equation

Temperature is computed by finite-difference methods. To do this, we define a regular grid in Ω (we use a grid finer by a factor of three than that employed to approximate the vector potential). The first and second order derivatives with respect to coordinates in the heat equation are approximated by central finite differences. The velocity in the heat equation is determined from (9) and (10).

We employ an implicit alternating-direction method [*Marchuk*, 1994] to compute temperature. Essentially, temperature T^{n+1} at time $t = t_{n+1}$ is found as

$$r^n = \tau \bigtriangledown^2 T^n + \mathbf{u} \cdot \bigtriangledown T^n, \quad \left[1 - \frac{\tau}{2}\frac{\partial^2}{\partial x_3^2}\right] T^* = r^n, \quad \left[1 - \frac{\tau}{2}\frac{\partial^2}{\partial x_2^2}\right] T^{**} = T^*,$$

$$\left[1 - \frac{\tau}{2}\frac{\partial^2}{\partial x_1^2}\right] T^{***} = T^{**}, \quad T^{n+1} = T^n + T^{***},$$

where τ is the time step. In the modeling, the parameter τ is chosen in such a way as to guarantee the stability of the finite difference method, namely:

$$\tau = \frac{1}{8}\frac{dx}{u_{max}}, \quad dx = [h_1^2 + h_2^2 + h_3^2]^{1/2}, \quad u_{max} = \max\{|u_i(x)| : x \in \overline{\Omega}, \quad i = 1, 2, 3\},$$

where $h_k = x_k^i - x_k^{i-1}$. To compute T^{n+1}, $n_2n_3 + n_1n_3 + n_1n_2$ tridiagonal systems are solved, and the corresponding number of independent modules can be organized to perform parallel computations of these systems by a tridiagonal method. The representation of the vector velocity potential based on cubic splines employed here makes it possible to compute both advection and diffusion of temperature simultaneously by finite-difference methods.

3.3. The Algorithm for Numerical Solution of the Inverse Problem of Mantle Convection

We define a uniform partition of the time axis at points $t_n = \vartheta_2 - \tau n$, where τ is the time step, and n successively takes integer values from 0 to some natural number $m = (\vartheta_2 - \vartheta_1)/\tau$. At each subinterval of time $[t_{n+1}, t_n]$, the solution of the problem backwards in time consists of the following basic steps.

Step 1. Given the temperature $T = T(t_n, \cdot)$ at $t = t_n$ we solve a set of linear algebraic equations derived from Eqs. (2) and (3) and the appropriate boundary conditions to find the velocity potential $\vec{\psi} = \vec{\psi}(t_n, \cdot)$.

Step 2. Eq. (9) is used to determine the velocity $\mathbf{u} = \mathbf{u}(t_n, \cdot; T)$, corresponding to temperature $T = T(t_n, \cdot)$, from the vector potential.

Step 3. The 'advective' temperature $T_a = T_a(t_{n+1}, \cdot)$ is determined by solving the advection heat equation (neglecting the diffusion term) backwards in time, and steps 1 and 2 are then repeated to find the velocity $\mathbf{u}_a = \mathbf{u}(t_{n+1}, \cdot; T_a)$, corresponding to the 'advective' temperature.

Step 4. The velocities $\mathbf{u}_a$ and $\mathbf{u}$ are used in the direct problem (Eq. (1) combined with the boundary conditions) and the conjugate problem (7), respectively, to find temperature $T = T(t_{n+1}, \cdot)$ at $t = t_{n+1}$.

Compared to our previous algorithm (Ismail-Zadeh et al., 2003a), step 3 is introduced here to accelerate the convergence of temperature iterations in solving the direct and conjugate heat problems (to satisfy inequality (8) in a few iterations at fixed ε).

After these algorithmic steps, we obtain temperature $T = T(t_n, \cdot)$, velocity potential $\vec{\psi} = \vec{\psi}(t_n, \cdot)$, and velocity $\mathbf{u} = \mathbf{u}(t_n, \cdot)$ corresponding to $t = t_n$, $n = 0, ..., m$. Based on the obtained results, we can use interpolation to reconstruct, when required, the entire process on the time interval $[\vartheta_1, \vartheta_2]$ in more detail. The time step is chosen automatically so that the maximal displacement of material points does not exceed a sufficiently small preset value.

Thus, at each subinterval of time we apply the variational method to the heat equation only, iterate the direct and conjugate problems for the heat equation in order to find temperature, and determine backward flow from the Stokes and continuity equations twice (for 'advective' and 'true' temperatures). Compared to the variational approach by *Bunge et al.* [2003], our numerical approach is computationally less expensive, because we do not involve the Stokes equation into the iterations between the direct and conjugate problems (the numerical solution of the Stokes equation is the most time consuming calculation). Moreover, our approach admits the use of temperature-dependent viscosity.

4. Restoration model of mantle plumes

In the modeling, we consider thermal plumes to be formed at the depth of 648 km, approximately the boundary between the lower mantle and upper mantle. To verify the validity of our numerical approach, we start our simulations by computing a forward model of the evolution of the thermal plumes and then we restore the evolved plumes to their earlier stages.

We assume the following dimensional model parameters: $\alpha = 3 \times 10^{-5}$ K^{-1}, $\Delta T = 2000$ K, $\rho_0 = 3.4 \times 10^3$ kg m^{-3}, and $\kappa = 0.8 \times 10^{-6}$ m^2 s^{-1} [*Schubert et al.,* 2001]; the reference mantle viscosity is $\mu_0 = 10^{21}$ Pa s [*Forte and Mitrovica*, 2001]; $h = 720$ km, and $l_1 = l_2 = 3h$, and therefore, the Rayleigh number is $Ra = 9.5 \times 10^5$. At initial time $t = 0$ we assume that the upper mantle temperature increases linearly with depth.

We consider the mantle viscosity μ to be temperature-dependent [*Busse et al.,* 1993]:

$$\mu(T) = \exp[Q/(T + G) - Q/(0.5 + G)],$$

where $Q = [225/\ln(r)] - 0.25\ln(r)$, $G = [15/\ln(r)] - 0.5$, and $r = 20$ is the effective viscosity ratio between the upper and lower boundaries of the model domain. The temperature dependence of this viscosity function is shown in Figure 1. We adopt this viscosity law for the sake of simplicity in the model and for benchmarking of our numerical codes [*Busse et al.,* 1993], although the methodology described here is valid for more general viscosity relationships [*Ismail-Zadeh et al.,* 2003a]. The chosen temperature (and depth) dependent viscosity profile has no minimum associated with the asthenospheric layer, while an inversion of the main convection-related geophysical data (free-air gravity, plate divergence, r.m.s. topography) suggests the existence of a low-viscosity channel at depths of 100 to 300 km with an average viscosity of about 10^{20} Pa s [*Forte and Mitrovica*, 2001]. A more realistic viscosity profile will influence the evolution of mantle plumes, but it will not affect results of the restoration of mantle plumes.

In order to initiate the growth of thermal plumes, we prescribe a small thermal perturbation on the horizontal plane $x_3 = 0.1$ (depth 648 km) at the initial time. The time the plumes take to develop depends on the amplitude of the initial perturbation. Hence, we computed the evolution of plumes to the stage presented in Fig. 2a and considered this stage as an initial configuration of the plumes in our forward modeling.

The model domain was divided into $37 \times 37 \times 29$ rectangular finite elements. The vector potential is approximated by tricubic splines on the elements, while temperature, velocity, and viscosity are represented on a more refined grid $112 \times 112 \times 88$. The evolution of the thermal plumes was modeled forward in time (Fig. 2, a-e). We interrupted the computations at a certain time (at 75 Myr), when the plumes had developed a mushroom geometry (Fig. 2*e*). The final state of the plumes in the forward model was used as the initial state of the plumes in backward (or restoration) models. In the following we refer to the final state of the thermal plumes in the forward modeling as the 'present' state of the plumes.

We apply the suggested numerical approach to restore the plumes from their 'present' state to the state they were in Late Cretaceous times (75 My ago). To achieve the accuracy $\varepsilon = 10^{-8}$ (see Eq. 8) we performed up to 10 iterations at each subinterval of time depending on the choice of the initial temperature guess, T_*. Despite the number of necessary iterations, a performance analysis demonstrated that the total execution time for the numerical restoration of the evolution of the plumes was only about a factor of 3 (depending on the number of iterations) larger than the time required for the forward modeling of the plumes. The restoration method developed by *Bunge et al.* [2003] is an order of magnitude more computationally expensive.

Figure 3 (left panel) shows the restored states of the plumes and the temperature residuals δT

$$\delta T(x_1, x_2) = \left[\int_0^{l_3} \left(T(x_1, x_2, x_3) - \tilde{T}(x_1, x_2, x_3) \right)^2 \mathrm{d}x_3 \right]^{1/2}$$

between the temperature $\tilde{T}$ predicted by the forward model and the temperature T restored to the same age. The temperature residuals are within a thousandth of a degree for the initial restoration period (from present to about 26 Myr), and the maximum residual reaches about $\delta T = 25°$ at the restoration time of 75 Myr. The computations show that the errors (temperature residuals) get larger the farther restorations move backwards in time. For the heat problem, it was shown that the size of time domain enters into the estimation of the rate of convergence, and hence this size influences the errors.

To demonstrate effects of heat diffusion (and its absence) on the temperature restoration, we computed the thermal plumes backwards in time using the heat advection equation (with no heat diffusion). The right panel of Fig. 3 presents the results of the modeling. The shapes of the restored mantle plumes become notably different from that of 'true' plumes (plumes modeled forwards in time) after 26 My. The temperature residuals (with no heat diffusion considered) are one to three orders of magnitude larger than those when heat diffusion is considered, and the minimum residual is about 100 K at the restoration time of 75 My. Thus, we have demonstrated that the neglect of heat diffusion in the backward modeling leads to an inaccurate restoration of mantle plumes.

Even though the coefficient of heat diffusion is small, the neglect of diffusion in the heat equation results in a different solution to the heat problem because of the reduction in the order of the differential equation [*Tikhonov and Samarskii,* 1990]. Moreover, when mantle convection is computed forwards in time using the heat diffusion equation and diffusion is ignored in the backward modeling of the same mantle convection, results are inconsistent and even unphysical.

The comparison between 'true' (modeled forwards in time) and restored (modeled backwards in time) plumes is quite natural from the computational point of view, but not from the geophysical point of view, because the mantle structure in the past (initial 'true' plumes) is unknown. Hence, we perform another numerical experiment on the accuracy of the restoration technique. We start from the 'present' structure of the plumes, apply the suggested technique to restore the past structure, run a forward model of the restored plumes, and compare the 'present' structure and the one recovered after the forward modeling. Figure 4 presents the results of this modeling which show that the restoration works quite well: temperature residuals (difference between the temperature of the restored mantle plumes and that of the plumes of the same age in the forward model) are within hundredths of a degree.

We have also performed similar computations with the heat diffusion equation replaced by the heat advection equation during the backward modeling. Figure 5 shows the results of restoration of the 'present' state of the plumes to 75 Myr ago and upbuilding of the restored plumes to the present time. The temperature residuals are larger (by several orders of magnitude) than those for the case when diffusion is considered in the backward modeling. Remarkably, the upbuilt 'present' state of the plumes in these two cases (with and without diffusion in backward modeling) are very similar in appearance, giving the false impression that reconstructions are satisfactory even with zero diffusion. Our analysis demonstrates that (i) the 'present' structures restored to the past are different for these two cases and (ii) the restoration errors (temperature residuals) are large when diffusion is neglected compared to when diffusion is included in the heat transfer.

5. Discussion

Conduction and convection are two major mechanisms for the transfer of heat. Conductive heat transfer in the mantle is a diffusion process occurring due to collision of molecules which transmit their kinetic energy to other molecules. Convective heat transfer is associated with the mantle motion due to gravity and plays a dominant part in the general transport of heat from the deep interiors of the Earth to the surface.

If the heat diffusion is negligible, the thermal convection in the mantle is time-reversible. "If you have a lot of particles doing something, and then you suddenly reverse the speed, they will completely undo what they did before ... If I reverse the time, the forces are not changed, and so the changes in velocity are not altered at corresponding distances. So each velocity then has a succession of alterations made in exactly the reverse of the way that they were made before, and it is easy to prove that the law of gravitation is time-reversible". With these words, the famous physicist R. Feynman introduced the time reversibility in gravity problems during the Messenger lectures on the character of physical laws he delivered at Cornell University in 1964 (Feynman, 1965).

The conductive heat transfer (heat diffusion) is a more complicated phenomenon. It is practically impossible to collect diffused heat back to the place from where it was diffused. Consider a simple example. If a 'cold' room is heated by a heater installed in the room, it becomes warmer in a few hours in the room. If the heater is switched off, it is ridiculous to expect that the diffused heat will return back to the heater or we could estimate the initial temperature of the heater from the current room's temperature.

Similar processes occur in the Earth. The mantle is heated from the core and from inside due to decay of radioactive elements. Since mantle convection is described by heat advection and diffusion, one can ask: is it possible to tell, from the 'present' temperature estimations of the Earth, something about the Earth's temperature in the geological past?

Even though heat diffusion is irreversible in the physical sense, we can accurately predict the heat transfer backwards in time using mathematical description of backward heat advection and diffusion without contradicting the basic thermodynamic laws. In this paper we have suggested a numerical method for modeling the backward heat equation in order to solve the inverse problem of thermal convection in the mantle. We do not solve directly the approximate backward heat equation, but rather we search for initial temperature conditions for the approximate forward heat equation.

There is a major physical limitation of the restoration of mantle plumes. If a thermal feature created, let say, a billion years ago by a boundary layer instability has completely diffused away by the present, it is impossible to restore the feature which was more prominent in the past. The time to which a present thermal structure in the upper mantle can be restored should be restricted by *the characteristic thermal diffusion time*, the time when the temperatures of the evolved structure and the ambient mantle are nearly not distinguished: $\tau_{dif} = d_{dif}^2/36\kappa$, where d_{dif} is the diffusion distance (see Turcotte and Schubert (2002); p. 155, Eq. 4-113 at $T \rightarrow T_1$, where T_1 is the ambient temperature). Given d_{dif}=650 km (the upper mantle thickness), the time of restoration should be limited to about 470 My.

A part of the geophysical community may maintain a skepticism about the inverse modeling of thermal convection. This skepticism may partly have its roots in our poor knowledge of the Earth's present structure and its physical properties which cannot allow for rigorous numerical paleoreconstructions of the Earth's evolution. Even considering simplified present-day structure and thermal state of the Earth, the backward modeling of thermomechanical evolution of the Earth is a computational challenge and several numerical problems (e.g., restorations to the deep past, about 400 My; more realistic rheology; temperature-dependent thermal diffusivity; etc.) should be solved before the technique become applicable for whole mantle convection reconstruction. An increasing accuracy of seismic tomography inversions and geodetic measurements, improving knowledge of gravity and geothermal fields, and precise laboratory experiments on physical and chemical properties of mantle rocks lead to better knowledge of the Earth, its structure and properties.

Physicists like to think that all you have to do is say: 'These are the conditions, now what happens next?' (Feynman, 1965), and hence the physicists prefer a forward modeling of phenomena. On the other hand, geologists like to predict a geological evolution based on discoveries on the Earth's surface, and therefore they prefer a modeling backwards in time. In geophysics these two approaches (forward and backward modeling) can be combined using applied mathematics as a tool in numerical modeling of the thermoconvective evolution of the Earth.

We have shown in this paper that a prominent present-day thermal feature in the mantle can be traced back into the geological past. A mathematical model of the thermal convection in the Earth's mantle is described by a set of equations, and we have demonstrated here that the set of equations can be solved numerically backwards in time. Our restoration methodology works well for the mathematical model, and we show its efficiency in the framework of this model.

6. Conclusions

The essential motivation for this research comes from the rapid progress made by seismic tomographers in imaging deep Earth structure. Restoration of seismically imaged structures backwards in time could provide an important way to test a range of geodynamic hypotheses. We have suggested a variational approach to the numerical solution of the inverse problem of thermal convection with infinite Prandtl number. We have tested the numerical approach by restoring a model of thermal plumes. The results of the restoration models together with the error estimates demonstrate the practicality of the suggested technique. We have also demonstrated that restored 'present' structures are different when heat diffusion is neglected. The restoration errors (temperature residuals) are large when diffusion is neglect.

The current solution algorithm for the inverse modeling of thermal convection allows us to restore temperature for about a hundred million years into the past based on the knowledge of the present temperature distribution in the mantle. This algorithm does not allow for the thermal restoration of the upper mantle to an age of several hundred million years (within the limit of the characteristic thermal diffusion time). This is associated with a coarseness of the grid used in modeling of the heat equation, and we are working on improvement of the algorithm in this part.

Besides the applicability of the backward modeling technique to problems of mantle plume and lithospheric slab restorations, the technique can be employed in predictions of paleotemperatures in sedimentary basins. The temperature estimations in the geological past can help in the forecasting of hydrocarbon generation, maturation, migration, and location in the basins.

The suggested numerical algorithm can be incorporated into many existing mantle convection codes in order to simulate the evolution of mantle structures backwards in time. The methodology opens a new possibility for restoration of mantle plumes, subducting lithosphere, plate movements, and thermoconvective mantle flow in general. Of course, real mantle plumes display more complex patterns and evolution, but our simple models represent an essential step in understanding how mantle plumes (and other mantle structures) might be reconstructed to the past.

Acknowledgments. We are grateful to P. Connolly, B. Naimark, H. Schmeling, and B. Steinberger for useful discussions and comments on the manuscript. This research was supported by NSF (EAR 01-05945), RFBR (02-01-00354) and the program "Deep Structure of the Earth's Interior" of the Department of Earth Sciences, Russian Academy of Sciences.

References

Ahlberg, J. H., E. H. Nilson, and J. L. Walsh, *The Theory of Splines and Their Applications,* 284 pp., Academic Press, New York, London, 1967.

Ames, K.A., and Epperson, J.F., A kernel-based method for the approximate solution of backward parabolic problems, *SIAM J. Numer. Anal., 34(4),* 1357–1390, 1997.

Bunge, H.-P., Hagelberg, C.R., and Travis, B.J., Mantle circulation models with variational data assimilation: Inferring past mantle flow and structure from plate motion histories and seismic tomography, *Geophys. J. Int., 152*, 280-301, 2003.

Busse, F.H., et al., 3D convection at infinite Prandtl number in Cartesian geometry – a benchmark comparison, *Geophys. Astrophys. Fluid Dynamics, 75,* 39–59, 1993.

Buzbee B.L., and Carasso A., On the numerical computation of parabolic problems for preceding times, *Math. Comput., 27*, 237–266, 1973.

Chandrasekhar, S. *Hydrodynamic and Hydromagnetic Stability,* 654 pp., Oxford University Press, Oxford, 1961.

Colton, D., The approximation of solutions to the backwards heat equation in a nonhomogeneous medium, *J. Math. Anal. Appl., 72*, 418–429, 1979.

Conrad, C.P., and Gurnis, M., Seismic tomography, surface uplift, and the breakup of Gondwanaland: Integrating mantle convection backwards in time, *Geochem. Geophys. Geosys., 4(3),* doi:10.1029/2001GC000299, 2003.

Elden, L., Time discretization in the backward solution of parabolic equations, *Math. Comput., 39,* 53–84, 1982.

Feynman, R. *The Character of Physical Law*, 173 pp., BBC, London, 1965.

Forte, A.M., and Mitrovica, J.X., Deep-mantle high-viscosity flow and thermochemical structure inferred from seismic and geodynamic data, *Nature, 410,* 1049–1056, 2001.

Goes, S., Govers, R., and Vacher, P., Shallow mantle temperatures under Europe from P and S wave tomography, *J. Geophys. Res., 105,* 11,153–11,169, 2000.

Grand, S.P., van der Hilst, R.D., and Widiyantoro, S., Global seismic tomography a snapshot of convection in the mantle, *GSA Today, 7*, 1–7, 1997.

Hadamard, J., *Lectures on the Cauchy Problem in Linear Partial Differential Equations*, 316 pp., Yale University Press, New Haven, 1923.

Ismail-Zadeh, A.T., A time-inverse problem of gravitational instability: numerical approach and applications, *Geophys. Res. Abstr., 1(1),* 61, 1999.

Ismail-Zadeh, A.T., Korotkii, A.I., and Tsepelev, I.A., Numerical approach to solving problems of slow viscous flow backwards in time, in: Proceedings of the Second M.I.T. Conference on Computational Fluid and Solid Mechanics, Boston, 16 to 20 June 2003, K.J. Bathe (Ed.), Elsevier Science, Amsterdam, pp. 602–605, 2003b.

Ismail-Zadeh, A.T., Talbot, C.J., and Volozh, Y.A., Dynamic restoration of profiles across diapiric salt structures: numerical approach and its applications, *Tectonophysics, 337,* 21–36, 2001a.

Ismail-Zadeh, A.T., Korotkii, A.I., Naimark, B.M., and Tsepelev, I.A., Numerical simulation of three-dimensional viscous flows with gravitational and thermal effects, *Comput. Math. Mathem. Phys., 41(9),* 1331–1345, 2001b.

Ismail-Zadeh, A.T., Korotkii, A.I., Naimark, B.M., and Tsepelev, I.A., Three-dimensional numerical simulation of the inverse problem of thermal convection, *Comput. Math. & Math. Phys., 43(4),* 587–599, 2003a.

Ismail-Zadeh, A.T., Korotkii, A.I., Naimark, B.M., Suetov, A.P., and Tsepelev, I.A., Implementation of a three-dimensional hydrodynamic model for evolution of sedimentary basins, *Comput. Math. & Math. Phys., 38(7),* 1138–1151, 1998.

Kaus, B.J.P., and Podladchikov, Y.Y., Forward and reverse modeling of the three-dimensional viscous Rayleigh-Taylor instability, *Geophys. Res. Lett.,* , *28,* 1095–1098, 2001.

Kirsch, A., *An Introduction to the Mathematical Theory of Inverse Problems,* 282 pp., Springer-Verlag, New York, 1996.

Korotkii, A.I., Tsepelev, I.A., Ismail-Zadeh, A.T., and Naimark, B.M., Three-dimensional backward modeling in problems of Rayleigh-Taylor instability, *Izvestiya/Proceedings of the Ural State University, 22(2),* 94–102, 2002.

Lu, H., Galerkin and weighted methods for a forward-backward heat equation, *Numer. Math., 75,* 339–365, 1997.

Marchuk, G.I., *Numerical Methods and Applications*, 272 pp., CRC Press, Boca Raton, 1994.

Moszynski, K., Approximation with frequency filter for backward parabolic equations, *Numer. Math., 88,* 159–183, 2001.

Ritsema, J., and Allen, R.M., The elusive mantle plume, *Earth Planet. Sci. Lett., 207,* 1–12, 2003.

Schubert, G., Turcotte, D.L., and Olson, P., *Mantle Convection in the Earth and Planets,* 940 pp., Cambridge University Press, Cambridge, 2001.

Sobolev, S.V., Zeyen, H., Stoll, G., Werling, F., Altherr, R., and Fuchs, K., Upper mantle temperatures from teleseismic tomography of French Massif Central including effects of composition, mineral reactions, anharmonicity, anelasticity and partial melt, Earth Planet. Sci. Lett., 139, 147–163, 1996.

Steinberger, B., and O'Connell, R.J., Changes of the earths rotation axis owing to advection of mantle density heterogeneities, *Nature, 387,* 169-173, 1997.

Steinberger, B., and O'Connell, R.J., Advection of plumes in mantle flow: implications for hotspot motion, mantle viscosity and plume distribution, *Geophys. J. Int., 132,* 412–434, 1998.

Tsepelev, I.A., Korotkii, A.I., Ismail-Zadeh, A.T., and Naimark, B.M., Parallel algorithms for modelling of thermal convection in viscous fluid (in Russian), in: Algorithms and software for parallel computations, Issue 4, O.N. Ulianov (Ed.), pp. 252–279, Institute of Mathematics and Mechanics, Ural Branch of the Russian Academy of Sciences, Ekaterinburg, 1999.

Tikhonov, A.N., and Arsenin V.Y., *Solution of Ill-Posed Problems,* 258 pp., Winston, Washington, D.C., 1977.

Tikhonov, A.N., and Samarskii, A.A., *Equations of Mathematical Physics*, 765 pp., Dover Publications, New York, 1990.

Turcotte, D.L., and Schubert, G., *Geodynamics*, 2nd ed., 456 pp., Cambridge University Press, Cambridge, 2002.

Vasiliev, F.P., *Methody optimizatsii* (in Russian), 824 pp., Factorial Press, Moscow,2002.

van der Voo, R., Spakman, W., and Bijwaard, H., Mesozoic subducted slabs under Siberia, *Nature, 397*, 246–249, 1999.

A. Ismail-Zadeh, International Institute of Earthquake Prediction Theory and Mathematical Geophysics, Russian Academy of Sciences, Warshavskoye shosse 79-2, Moscow 113556, Russia; and Geophysical Institute, University of Karlsruhe, Hertzstr. 16, Karlsruhe 76187, Germany (e-mails: aismail@mitp.ru; Alik.Ismail-Zadeh@gpi.uni-karlsruhe.de)

G. Schubert, Department of Earth and Space Sciences, Institute of Geophysics and Planetary Physics, University of California at Los Angeles, 3806 Geology Building, 595 Charles Young Drive East, Los Angeles, CA 90095-1567 (e-mail: schubert@ucla.edu)

A. Korotkii, and I. Tsepelev, Institute of Mathematics and Mechanics, Ural Branch, Russian Academy of Sciences, ul. S. Kovalevskoy 16, Ekaterinburg 620219, Russia (e-mail: Korotkii@imm.uran.ru; Tsepelev@imm.uran.ru)

Received ____________________

Appendix 1. On the stability of the solution to the one-dimensional backward diffusion equation

Consider the following boundary-value problem for the 1-D backward diffusion equation:

$$\partial u(t,x)/\partial t = \partial^2 u(t,x)/\partial x^2, \qquad 0 \le x \le \pi, \quad t \le 0,$$

$$u(t,0) = 0 = u(t,\pi), \qquad t \le 0,$$

$$u(0,x) = \phi_n(x), \qquad 0 \le x \le \pi.$$

At the initial time we assume that the function $\phi_n(x)$ takes the following two forms:

$$\phi_n(x) = \frac{1}{4n+1}\sin((4n+1)x)$$

and

$$\phi_0(x) \equiv 0.$$

Note that

$$\max_{0\le x\le\pi} |\phi_n(x) - \phi_0(x)| \le \frac{1}{4n+1} \to 0 \qquad \text{at} \quad n \to \infty.$$

The following two solutions of the problem correspond to the two chosen functions of $\phi_n(x)$, respectively:

$$u_n(t,x) = \frac{1}{4n+1}\exp(-(4n+1)^2 t)\ \sin((4n+1)x) \qquad \text{at} \quad \phi_n(x) = \phi_n.$$

and

$$u_0(t,x) \equiv 0 \qquad \text{at} \quad \phi_n(x) = \phi_0$$

At $t = -1$ and $x = \pi/2$ we obtain

$$u_n(-1,\pi/2) = \frac{1}{4n+1}\exp((4n+1)^2) \to \infty \qquad \text{at} \quad n \to \infty.$$

At large n two closely set initial functions ϕ_n and ϕ_0 are associated with the two strongly different solutions at $t = -1$ and $x = \pi/2$. Hence, a small error in the initial data can result in very large errors in the solution to the backward problem, and therefore the solution is unstable, and the problem is ill-posed.

Appendix 2. Derivation of the gradient of objective functional J

We consider the objective functional defined by (4) and determine the gradient of the functional (see *Ismail-Zadeh et al.* [2003a] for more details). An increment of the functional can be represented in the form:

$$J(\varphi + h) - J(\varphi) = \int_\Omega |T(\vartheta_2, x; \varphi + h) - \chi(x)|^2 dx - \int_\Omega |T(\vartheta_2, x; \varphi) - \chi(x)|^2 dx =$$

$$= 2\int_\Omega (T(\vartheta_2, x; \varphi) - \chi(x)) z(\vartheta_2, x) dx + \int_\Omega z(\vartheta_2, x)^2 dx,$$

where $h(x)$ is a small heat increment to the unknown initial temperature $\varphi(x)$, and $z = T(t, x; \varphi + h) - T(t, x; \varphi)$ is the solution to the following forward heat problem

$$\begin{aligned} &\partial z/\partial t + \mathbf{u} \cdot \nabla z - \nabla^2 z = 0, && x \in \Omega, \quad t \in (\vartheta_1, \vartheta_2), \\ &\sigma_1 z + \sigma_2 \partial z/\partial \mathbf{n} = 0, && x \in \Gamma, \quad t \in (\vartheta_1, \vartheta_2), \\ &z(\vartheta_1, x) = h(x), && x \in \Omega. \end{aligned} \tag{11}$$

We show below that

$$2\int_\Omega (T(\vartheta_2, x; \varphi) - \chi(x)) z(\vartheta_2, x) dx = \int_\Omega \Psi(\vartheta_1, x) h(x) dx,$$

where $\Psi(t, x) = 2(T(t, x; \varphi) - \chi(x))$ is the solution to the conjugate boundary problem (7). Indeed,

$$\int_\Omega \Psi(\vartheta_2, x) z(\vartheta_2, x) dx = \int_\Omega \int_{\vartheta_1}^{\vartheta_2} \frac{\partial}{\partial t} \left(\Psi(t, x) z(t, x) \right) dx dt + \int_\Omega \Psi(\vartheta_1, x) h(x) dx.$$

Considering the fact that $\Psi = \Psi(t,x)$ and $z = z(t,x)$ are the solutions to (7) and (8) respectively, and the velocity $\mathbf{u}$ satisfies Eq.(3) and the boundary conditions specified, we obtain

$$\int_\Omega \int_{\vartheta_1}^{\vartheta_2} \frac{\partial}{\partial t}(\Psi(t,x)z(t,x))dtdx = \int_{\vartheta_1}^{\vartheta_2} \int_\Omega \left\{ \frac{\partial}{\partial t}\Psi(t,x)z(t,x) + \Psi(t,x)\frac{\partial z(t,x)}{\partial t} \right\} dxdt =$$

$$= \int_{\vartheta_1}^{\vartheta_2} \int_\Omega z(t,x)\left[-\mathbf{u}\cdot \bigtriangledown \Psi - \bigtriangledown^2 \Psi \right] dxdt + \int_{\vartheta_1}^{\vartheta_2} \int_\Omega \Psi(t,x) \left[-\mathbf{u}\cdot \bigtriangledown z + \bigtriangledown^2 z \right] dxdt =$$

$$= \int_{\vartheta_1}^{\vartheta_2} \int_\Gamma \{\Psi \ \bigtriangledown z\cdot \mathbf{n} - z\ \nabla\Psi\cdot \mathbf{n}\}\, d\Gamma dt + \int_{\vartheta_1}^{\vartheta_2} \int_\Omega \{\bigtriangledown\Psi\cdot\bigtriangledown z - \bigtriangledown z\cdot\bigtriangledown\Psi\}\, dxdt +$$

$$+ \int_{\vartheta_1}^{\vartheta_2} \int_\Omega \{z\Psi\ \nabla\cdot\mathbf{u} + \Psi\ \mathbf{u}\cdot\bigtriangledown z - \Psi\ \mathbf{u}\cdot\bigtriangledown z\}\, dxdt - \int_{\vartheta_1}^{\vartheta_2} \int_\Gamma z\Psi\, \mathbf{u}\cdot\mathbf{n}\, d\Gamma dt = 0.$$

Hence, we can derive that:

$$J(\varphi + h) - J(\varphi) = \int_\Omega \Psi(\vartheta_1, x)h(x)dx + \int_\Omega z(\vartheta_2,x)^2 dx = \int_\Omega \Psi(\vartheta_1,x)h(x)dx + o(\|h\|).$$

And therefore, we obtain that the gradient of the objective functional is represented as

$$\bigtriangledown J(\varphi) = \Psi(\vartheta_1, \cdot).$$

Figure 1. Temperature-dependent viscosity used in the modeling.

Figure 2. Mantle plumes in the forward modeling at successive times: from 75 Myr ago (a) to the 'present' state of the plumes (e). The plumes are represented here and in Figs. 3 to 5 by isothermal surfaces at 1840 K.

Figure 3. Restored mantle plumes in the backward modeling and restoration errors (temperature residuals) at successive times: from the 'present' to 75 Myr ago. The left two panels present the model results in the case when diffusion is included in the heat transfer, and the right two panels are for the case in which diffusion is neglected.

Figure 4. Mantle plumes restored from the 'present' to 75 Myr ago (left panel), upbuilt plumes back to their 'present' state (central panel), and the restoration errors (right panel) in the case when diffusion is included.

Figure 5. Mantle plumes restored from the 'present' to 75 Myr ago (left panel), upbuilt plumes back to their 'present' state (central panel), and the restoration errors (right panel) in the case when diffusion is neglected.

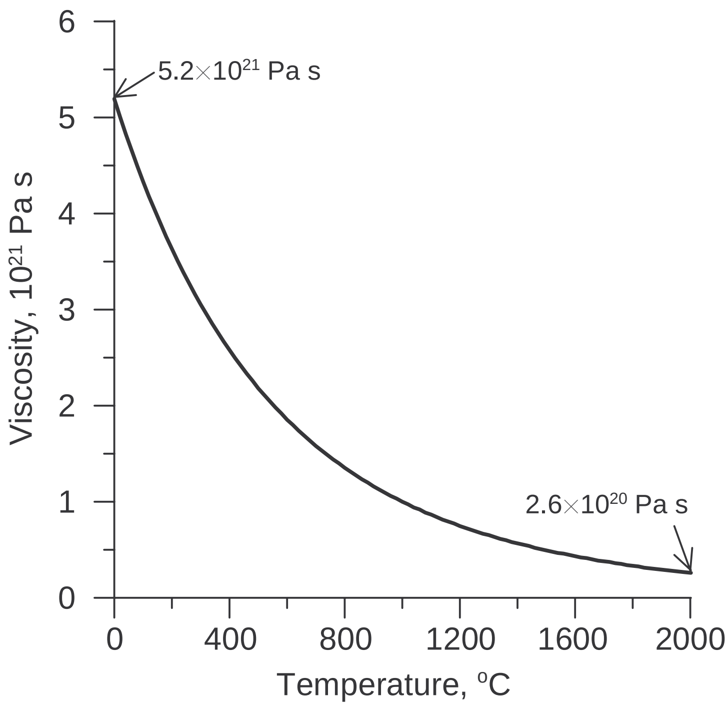

5.2×10²¹ Pa s
2.6×10²⁰ Pa s
Viscosity, 10²¹ Pa s
0
1
2
3
4
5
6
0
400
800
1200
1600
2000
Temperature, °C

Fig. 1

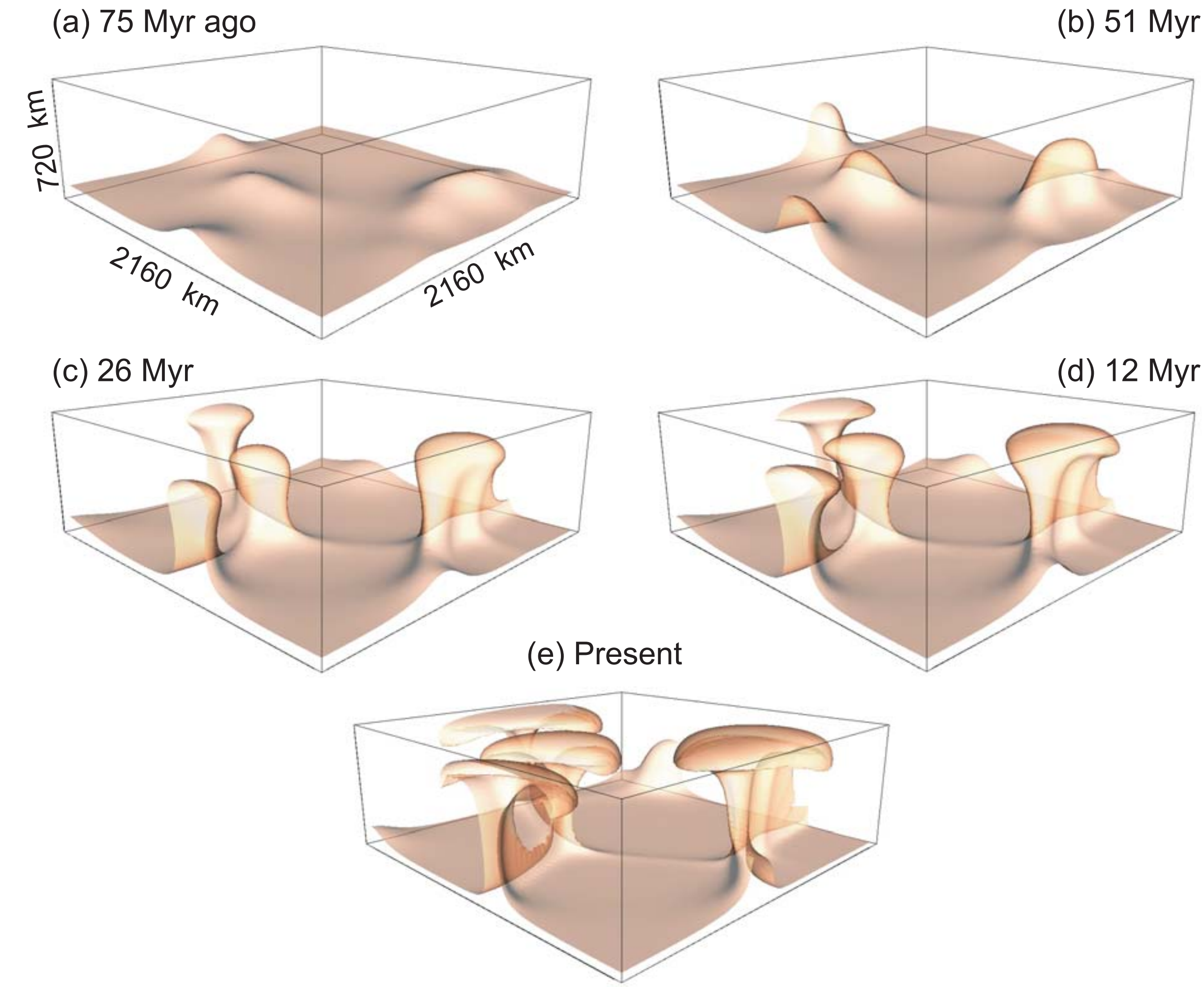
(a) 75 Myr ago
720 km
2160 km
2160 km
(b) 51 Myr
(c) 26 Myr
(d) 12 Myr
(e) Present

Fig. 2

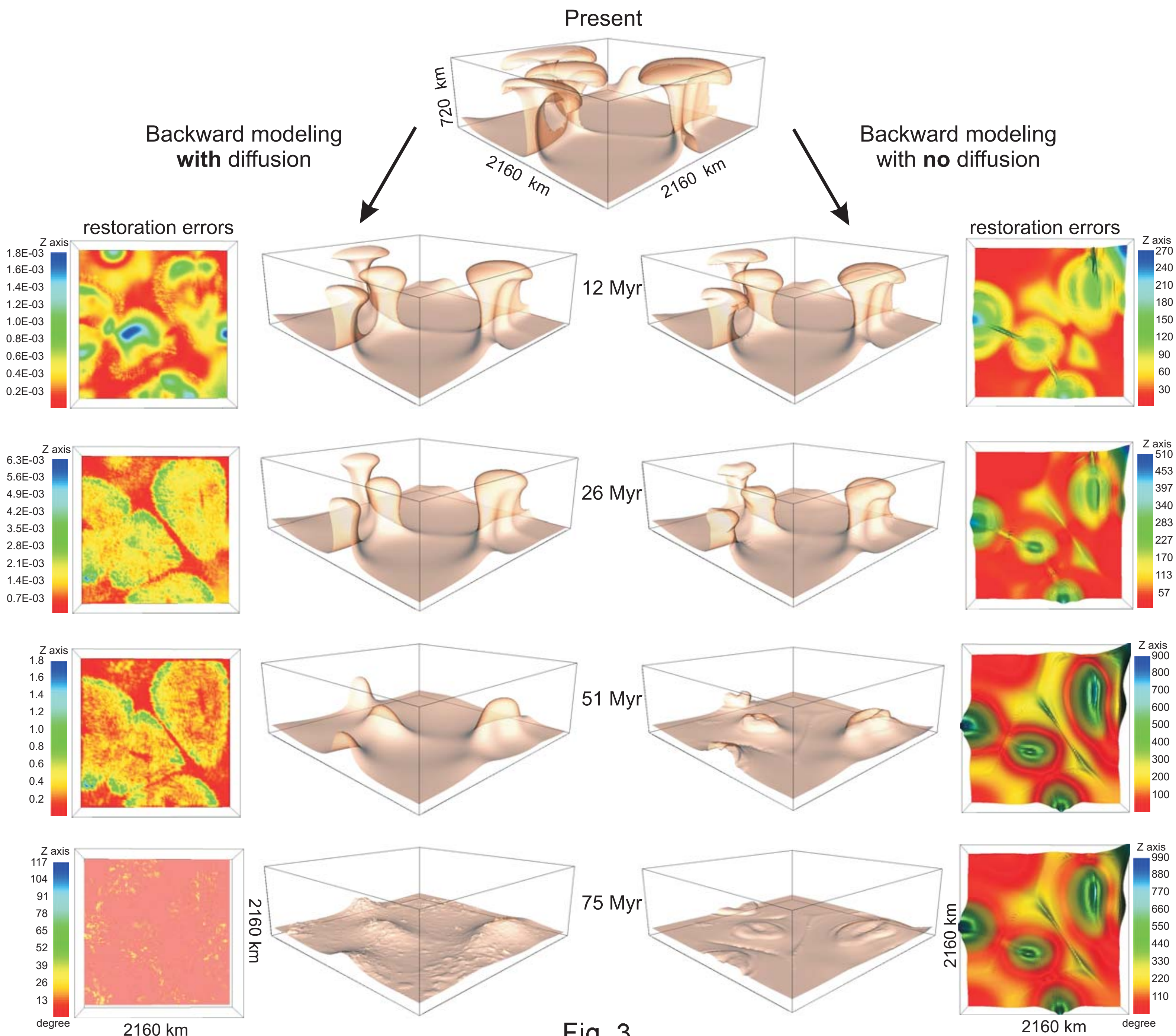
Present
720 km
2160 km
2160 km
Backward modeling
with diffusion
Backward modeling
with no diffusion
restoration errors
restoration errors
12 Myr
26 Myr
51 Myr
75 Myr
Z axis
1.8E-03
1.6E-03
1.4E-03
1.2E-03
1.0E-03
0.8E-03
0.6E-03
0.4E-03
0.2E-03
Z axis
6.3E-03
5.6E-03
4.9E-03
4.2E-03
3.5E-03
2.8E-03
2.1E-03
1.4E-03
0.7E-03
Z axis
1.8
1.6
1.4
1.2
1.0
0.8
0.6
0.4
0.2
Z axis
117
104
91
78
65
52
39
26
13
degree
2160 km
2160 km
Z axis
270
240
210
180
150
120
90
60
30
Z axis
510
453
397
340
283
227
170
113
57
Z axis
900
800
700
600
500
400
300
200
100
Z axis
990
880
770
660
550
440
330
220
110
degree
2160 km
2160 km

Fig. 3

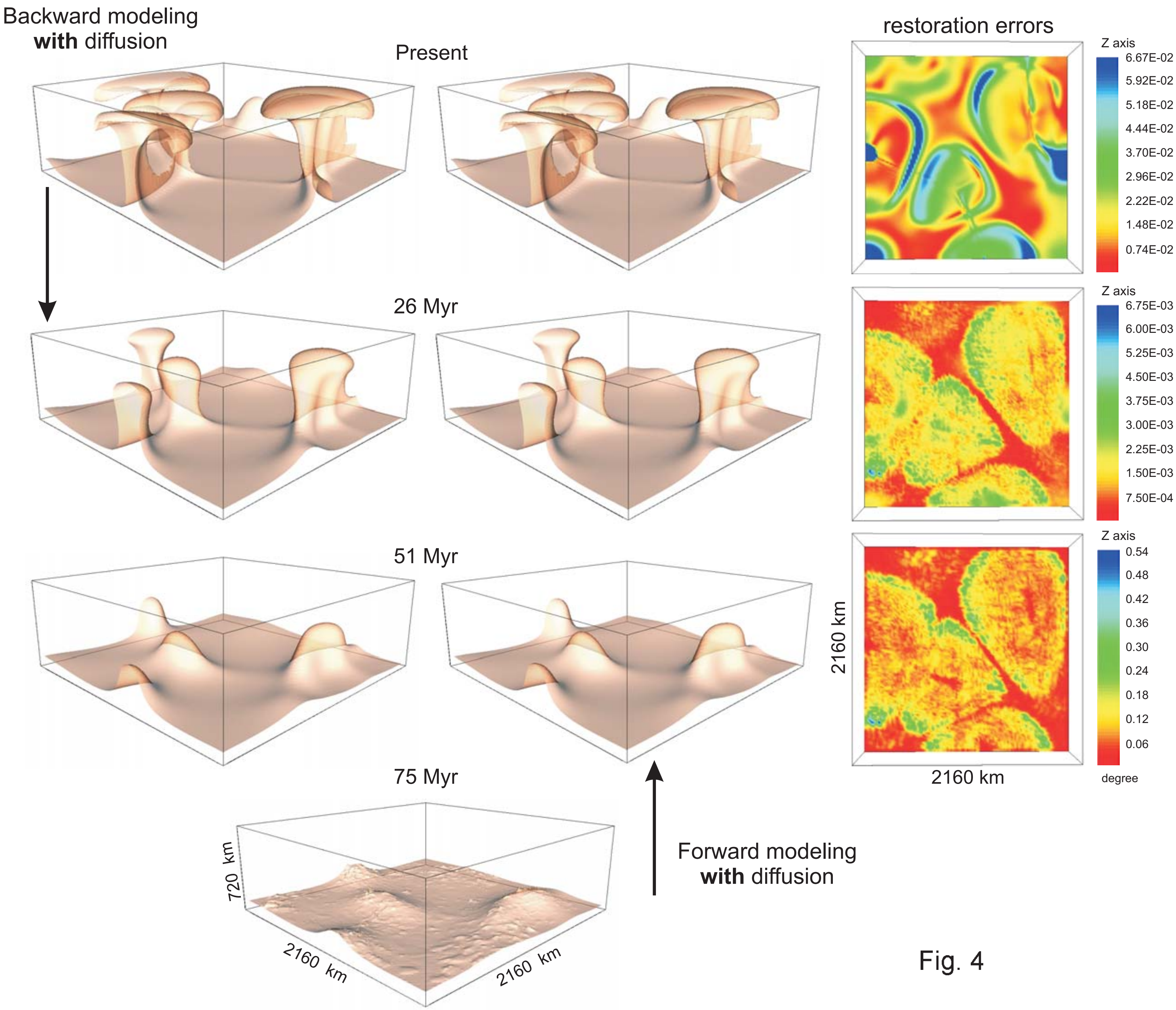
Backward modeling
with diffusion
Present
restoration errors
Z axis
6.67E-02
5.92E-02
5.18E-02
4.44E-02
3.70E-02
2.96E-02
2.22E-02
1.48E-02
0.74E-02
26 Myr
Z axis
6.75E-03
6.00E-03
5.25E-03
4.50E-03
3.75E-03
3.00E-03
2.25E-03
1.50E-03
7.50E-04
51 Myr
Z axis
0.54
0.48
0.42
0.36
0.30
0.24
0.18
0.12
0.06
degree
2160 km
2160 km
75 Myr
720 km
2160 km
2160 km
Forward modeling
with diffusion

Fig. 4

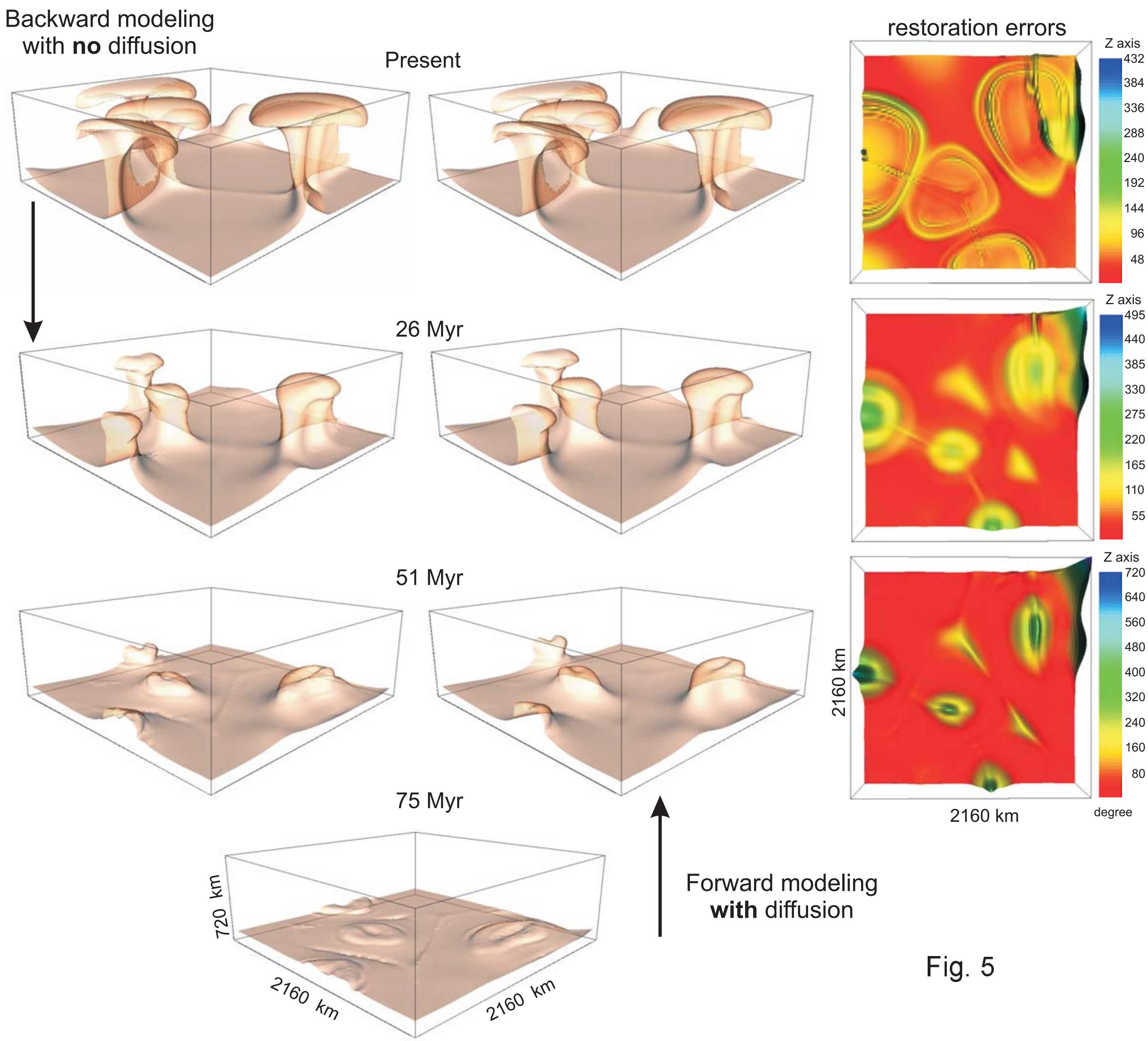

Backward modeling
with **no** diffusion
Present
26 Myr
51 Myr
75 Myr
720 km
2160 km
2160 km
Forward modeling
with diffusion
restoration errors
Z axis
432
384
336
288
240
192
144
96
48
Z axis
495
440
385
330
275
220
165
110
55
Z axis
720
640
560
480
400
320
240
160
80
2160 km
2160 km
degree

Fig. 5